ELSEVIER

Earth and Planetary Science Letters 205 (2003) 239–255

EPSL

www.elsevier.com/locate/epsl

Mechanisms of metal–silicate equilibration in the terrestrial magma ocean

D.C. Rubie [a,*], H.J. Melosh [b], J.E. Reid [a], C. Liebske [a], K. Righter [b]

[a] *Bayerisches Geoinstitut, Universität Bayreuth, 95440 Bayreuth, Germany*
[b] *Lunar and Planetary Laboratory, University of Arizona, Tucson, AZ 85721, USA*

Received 7 June 2002; received in revised form 11 September 2002; accepted 22 October 2002

Abstract

It has been proposed that the high concentrations of moderately siderophile elements (e.g. Ni and Co) in the Earth's mantle are the result of metal–silicate equilibration at the base of a deep magma ocean that formed during Earth's accretion. According to this model, liquid metal ponds at the base of the magma ocean and, after equilibrating chemically with the overlying silicate liquid at high pressure (e.g. 25–30 GPa), descends further as large diapirs to form the core. Here we investigate the kinetics of metal–silicate equilibration in order to test this model and place new constraints on processes of core formation. We investigate two models: (1) Reaction between a layer of segregated liquid metal and overlying silicate liquid at the base of a convecting magma ocean, as described above. (2) Reaction between dispersed metal droplets and silicate liquid in a magma ocean. In the liquid-metal layer model, the convection velocity of the magma ocean controls both the equilibration rate and the rate at which the magma ocean cools. Results indicate that time scales of chemical equilibration are two to three orders of magnitude longer than the time scales of cooling and crystallization of the magma ocean. In the falling metal droplet model, the droplet size and settling velocity are critical parameters that we determine from fluid dynamics. For likely silicate liquid viscosities, the stable droplet diameter is estimated to be $\sim$1 cm and the settling velocity $\sim$0.5 m/s. Using such parameters, liquid metal droplets are predicted to equilibrate chemically after falling a distance of $<$200 m in a magma ocean. The models indicate that the concentrations of moderately siderophile elements in the mantle could be the result of chemical interaction between settling metal droplets and silicate liquid in a magma ocean but not between a segregated layer of liquid metal and overlying silicate liquid at the base of the magma ocean. Finally, due to fractionation effects, the depth of the magma ocean could have been significantly different from the value suggested by the apparent equilibration pressure.

Keywords: core formation; accretion; differentiation; metal–silicate segregation; siderophile elements

1. Introduction

Formation of the metallic cores of the Earth and other planetary bodies occurred during accretion by the physical separation of metal from silicates. This process is likely to have involved the

* Corresponding author: Tel.: +49-921-553711; Fax: +49-921-553769.
E-mail address: dave.rubie@uni-bayreuth.de (D.C. Rubie).

0012-821X/02/$ – see front matter
PII: S0012-821X(02)01044-0

separation of liquid metal from either liquid silicate or crystalline silicates [1]. The first of these scenarios involves metal–silicate separation in a magma ocean (Fig. 1) as is likely to have been present on the Moon, Mars and possibly on Earth as a consequence of giant impacts [2,3].

Important evidence concerning core formation processes is provided by the chemistry of the Earth's mantle. In particular, the current concentrations of siderophile elements (iron-loving; e.g. Ni, Co, W) in the mantle are considered to have resulted largely from chemical interaction between metal and silicates during core formation. Based on metal–silicate partition coefficients for siderophile elements determined at 1 bar, the concentrations of these elements in the mantle are much too high (e.g. [4,5]). It has been proposed that this 'overabundance' of siderophile elements is the consequence of metal–silicate separation at high pressures and temperatures because partition coefficients, at least for some of the moderately siderophile elements, are greatly lowered under such conditions. Based on Ni, Co Mo, W and P partition coefficients, mantle concentrations of siderophile elements could be explained by high pressure and temperature equilibrium between metal and silicate in a magma ocean scenario [6–8]. Most of these studies, together with additional work [9,10], argue for an equilibrium signature in the mantle, set by liquid metal and liquid silicate at 25–30 GPa, 2100–2400 K, and an oxygen fugacity below the iron–wüstite (IW) buffer.

These conclusions, based solely on partitioning, have led to physical models in which a layer of liquid metal accumulates at the base of a silicate magma ocean ~700 km deep and chemically equilibrates there with the overlying convecting silicate liquid [6,8,11]. In an alternative scenario, small metal droplets equilibrated with the silicate liquid during gravitational settling immediately after the magma ocean formed [1,12,13].

In order to test the viability of these 'metal layer' and 'metal droplet' magma ocean models (Fig. 1), we explore the role of kinetics during metal–silicate equilibration. Although kinetics have been discussed for the case of metal droplets [12], the rate of equilibration between a layer of liquid metal and an overlying convecting magma ocean has not been considered previously. One particular question, relevant to both models, concerns the equilibration time scale relative to the time scale of magma ocean crystallization because the latter is very short, on the order of a few hundred years [11].

2. Magma ocean properties

With Rayleigh numbers (which provide a measure of the vigor of convective flow) in the range 10^{27}–10^{32}, a deep magma ocean undergoes turbulent convection with convection velocities on the order of several meters per second. We use a parameterized convection model [3,11] to estimate the convection velocity v_c, as required for the kinetic models discussed below, and for calculating the early cooling history of the magma ocean. The Rayleigh number is given by:

$$Ra = \frac{\rho_s \alpha g \Delta T z_s^3}{\kappa \eta} \quad (1)$$

where ρ_s is the density of the silicate magma, α is the coefficient of thermal expansion, g is the acceleration due to gravity, ΔT is the difference between the surface temperature T_s and the potential temperature, z_s is the depth of the magma ocean, κ is thermal diffusivity and η is the dynamic viscosity. This enables the Nusselt number (a measure of the relative importance of convective and conductive heat flow) to be calculated for hard turbulent convection:

$$Nu = 0.089 Ra^{\beta} \quad (2)$$

We assume that $\beta = 1/3$ (based on Kolmogorov scaling), although in reality its value is likely to be closer to 0.309 [14]. The convective velocity is then obtained as:

$$v_c = (\alpha g \kappa \Delta T)^{1/3} Nu^{1/3} \quad (3)$$

Finally, the rate of heat loss is given by:

$$q_{\mathrm{loss}} = Nuk\Delta T / z_s \quad (4)$$

where k is thermal conductivity.

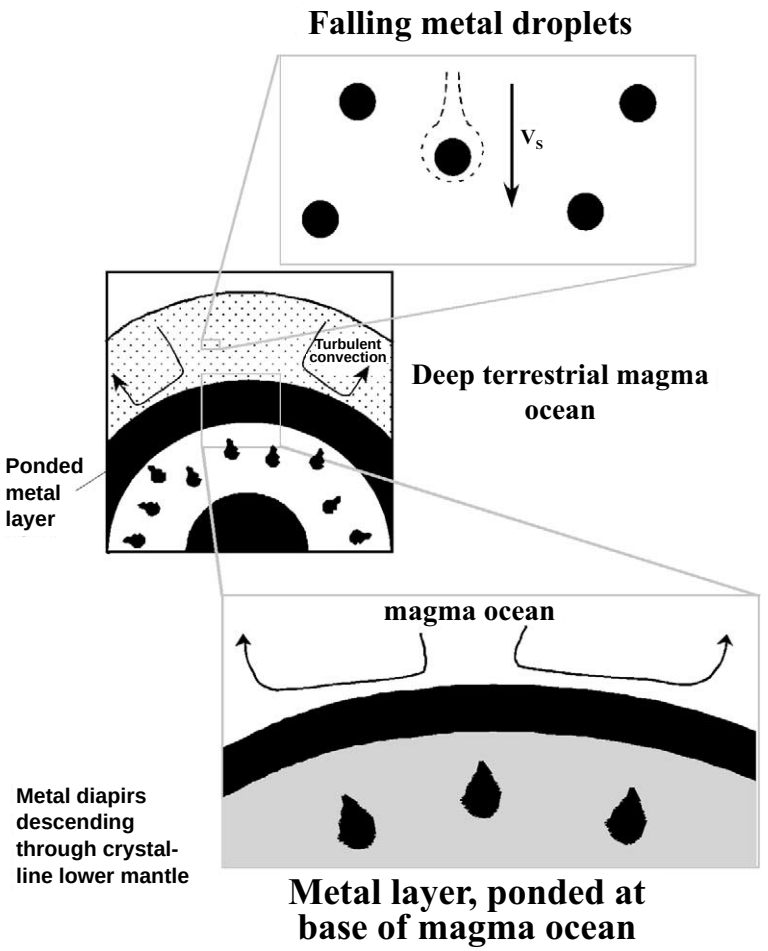

Fig. 1. Cartoon summarizing processes of metal–silicate separation during core formation. The central cartoon shows a deep magma ocean overlying crystalline lower mantle (white). Metal is separating from silicate liquid in the magma ocean in the form of small liquid metal droplets (top). A layer of liquid metal has collected at the base of the magma ocean and periodically descends further as large diapirs (bottom).

We assume that the rate of surface heat loss is controlled by radiation according to:

$$q_{\text{loss}} = \sigma_B \, T_s^4 \tag{5}$$

where σ_B is the Stefan–Boltzmann constant. A dense steam atmosphere, which may have surrounded the early Earth, greatly reduces the heat flux when T_s drops below 1500 K [11,15,16]. At higher surface temperatures the presence of a steam atmosphere has little effect on heat loss and T_s is determined by equating Eqs. 4 and 5. The temperature at the base of the magma ocean is assumed to be initially either on the peridotite liquidus or above the liquidus and is therefore defined by the magma ocean depth. This assumption avoids complexities of modeling flow and diffusion in partially crystalline magma. Liquidus temperatures up to 25 GPa are obtained from published phase diagrams [17] (based on data obtained up to 25 GPa) and [18,19] at higher pressures. The potential temperature at the Earth's surface is determined by calculating an adiabat (using thermodynamic data of [20]).

In order to describe transport properties of liquid metal and liquid silicate, we use the diffusion

Table 1
Values of physical parameters

Silicate liquid		Ref.
Density, ρ_s	3750 kg m^{-3}	[20]
Activation enthalpy for Si,O diffusion, H^*	267 kJ mol^{-1}	[21]
Activation volume for Si,O diffusion, V^*	0 kJ GPa^{-1} mol^{-1}	[21]
Pre-exponential for Si,O diffusion, D_0 [a]	1.5×10^{-2} m^2 s^{-1}	[21]
Oxygen jump distance, λ_O	2.8 Å	[21]
Thermal diffusivity, κ	10^{-6} m^2 s^{-1}	[35]
Thermal expansivity, α	6×10^{-5} K^{-1}	[36]
Heat capacity, C_p	10^3 J kg^{-1} K^{-1}	[11]
Latent heat of crystallization, L	4×10^5 J kg^{-1}	[3]
Initial Ni content, $C_s(0)$	42 ppm	[25]
Metal liquid		
Density, ρ_m	7800 kg m^{-3}	[37]
Activation enthalpy for Fe diffusion, H^*	100 kJ mol^{-1}	[34]
Activation volume for Fe diffusion, V^*	2.8 kJ GPa^{-1} mol^{-1}	[34]
Pre-exponential for Fe diffusion, D_0	1.7×10^{-5} m^2 s^{-1}	[34]
Initial Ni content, $C_m(0)$	32 700 ppm	[25]
Other parameters		
Metal–silicate distribution coefficient, D^{ms}	28	[32]
Metal–silicate interfacial energy, σ	1 N m^{-2}	[1]
Stefan–Boltzmann constant, σ_B	5.67×10^{-8} W m^{-2} K^{-4}	

[a] The value of D_0 is larger than that determined for $CaMgSi_2O_6$ liquid by a factor of 10, as explained in the text.

equation:

$$D = D_0 \exp(-(H^* + PV^*)/RT) \quad (6)$$

where D_0 is the pre-exponential term, H^* is the activation enthalpy, V^* is the activation volume, P is pressure and T is absolute temperature. The viscosity of silicate liquid is calculated using the Eyring relation [21,22]:

$$D_{Si,O} = \frac{k_B T}{\eta \lambda} \quad (7)$$

where $D_{Si,O}$ is the diffusion coefficient for Si or O, k_B is the Boltzmann constant, η is viscosity and λ is the jump distance of the diffusing ions (assumed to be 2.8 Å for silicate liquid). While values of most of the parameters in Eqs. 1–7 are reasonably well known (Table 1), the viscosity of peridotite liquid has not been determined experimentally. In addition, diffusivities of siderophile elements in peridotite liquid, which are required for the kinetic models presented below, have not been determined. We therefore base these parameters on the transport properties of $CaMgSi_2O_6$ (diopside composition) liquid, determined experimentally at high pressures (Fig. 2). Self-diffusivities of Si and O in $CaMgSi_2O_6$ liquid have been determined up to 17 GPa and 2700 K and viscosities up to 13 GPa and 2500 K [21,22]. Within experimental uncertainties, these properties are related by Eq. 7 [22]. Peridotite liquid is more depolymerized than $CaMgSi_2O_6$ liquid (NBO/T values are $\sim$2.7 and 2.0, respectively), which means that diffusion in peridotite liquid should be faster and the viscosity lower. We assume that chemical diffusivity in peridotite liquid is faster by a factor of 10 and viscosity is lower by a factor of 10 compared with $CaMgSi_2O_6$ liquid, the latter assumption being consistent with a preliminary viscosity determination at 7.5 GPa [22] (Table 1). Results show that the effects of pressure on diffusivity and viscosity of $CaMgSi_2O_6$ liquid are small, with these properties varying by a factor of only about $\pm$2 between 0 and 17 GPa [21]. We therefore assume that $V^* = 0$ in Eq. 6.

Preliminary results show that the diffusivities (D_S) of trace amounts of the siderophile elements

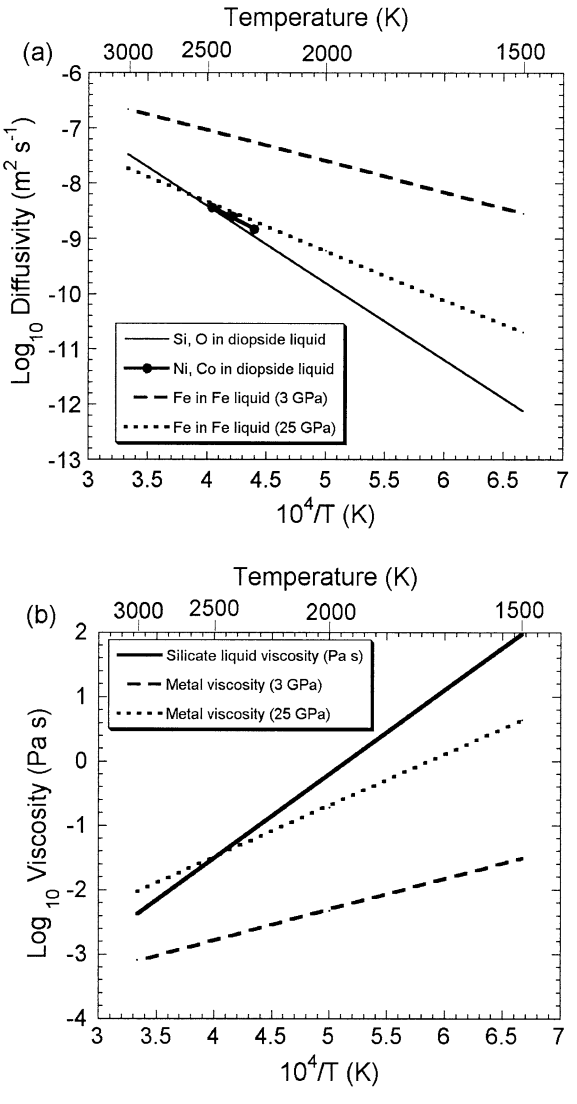

Fig. 2. Diffusivities (a) and viscosities (b) of $CaMgSi_2O_6$ and Fe liquids as a function of inverse temperature based on data of [21,22,33,34]. For peridotite liquid in a magma ocean, we assume that diffusivities are larger by a factor of 10 and viscosities lower by a factor of 10 compared with $CaMgSi_2O_6$ liquid.

Ni and Co in $CaMgSi_2O_6$ liquid at 4–8 GPa and 2300–2500 K [22] are faster than Si and O diffusivities ($D_{Si,O}$) by a factor of between 1 and 2, depending on temperature (Fig. 2). Below, we assume that $D_S = 2D_{Si,O}$ in the metal layer model and $D_S = D_{Si,O}$ in the metal droplet models (thus maximizing and minimizing the respective equilibration rates).

In the case of the metal layer model discussed below, equilibration between metal and silicate will cease as soon as the silicate magma immediately above the metal layer has crystallized. To estimate how long this takes, we calculate the cooling history of the magma ocean until the temperature at the metal–silicate interface has decreased to 200 K below the peridotite liquidus, which is equivalent to 20–100 K below the solidus [17]. The rate of heat loss is given by Eqs. 4 and 5 and the effects of latent heat of crystallization and heat capacity are included (Table 1). We assume that, on average, 50% crystallization develops linearly over the temperature range of the calculation and that the average effective magma viscosity is given by $\eta_{eff} = \eta \exp(23.03\phi)$ where η is the silicate liquid viscosity and ϕ is the average fraction of crystals present [3]. The viscosity, Rayleigh number, Nusselt number and rate of heat loss are calculated over a succession of small temperature increments (≤ 2 K) to determine the cooling history. We apply this model only to magma oceans with depths ≥ 400 km – the cooling rates of shallower magma oceans are dominated by crystallization (because of the topology of the peridotite phase diagram), are affected strongly by a steam atmosphere and are consequently relatively slow (e.g. [11]).

3. Thermal diffusion and fluid mechanics of chemical equilibration

The laws describing the diffusive exchange of atoms between one material and another are mathematically identical to those that describe the transfer of heat by conduction. There is a well-known proportionality between the rate at which heat is transferred and that at which mass is transferred [23]. Thus, the flux $\mathbf{q}$ of heat down a gradient in temperature T is given by Fourier's law:

$$\mathbf{q} = -k\nabla T \tag{8}$$

where $k = \rho c_P \kappa$ is thermal conductivity, ρ is den-

sity, c_P is heat capacity and κ is thermal diffusivity, measured in $m^2\ s^{-1}$. Similarly, the flux **F** of material down a gradient in mass concentration C is given by Fick's law:

$$\mathbf{F} = -D\nabla C \tag{9}$$

where D is the diffusion coefficient, also measured in $m^2\ s^{-1}$.

When heat is transferred between fluids, one or both of which may be moving, an important dimensionless parameter is the Prandtl number, N_{Pr}, which is the ratio between the kinematic viscosity ν and the thermal diffusivity κ, $N_{Pr} = \nu/\kappa$. Thus, the rate $\dot{Q}$ at which heat is transferred from a planar heated boundary of length L and area A to a laminar fluid moving past it at velocity v_f is [24]:

$$\dot{Q} = 0.664k(T_b - T_f)N_{Pr}^{1/3}Re_L^{1/2} \tag{10}$$

where T_b is the temperature of the boundary and T_f is the fluid temperature. In this expression Re_L is the Reynolds number of the flow along the plate, given by:

$$Re_L = \frac{v_f L}{\nu} \tag{11}$$

The heat transfer Eq. 10 applies to flows in which Re_L is less than about 4×10^5 and $N_{Pr} > 0.6$. None of the cases that we consider in this paper lie outside of these limits.

By analogy, the rate $\dot{M}$ of material transfer from the boundary to the fluid is given by:

$$\dot{M} = 0.664D(C_b - C_f)N_{Sc}^{1/3}Re_L^{1/2} \tag{12}$$

where N_{Sc} is the 'Schmidt' number ([23], p. 250), which is analogous to the Prandtl number. The dimensionless Schmidt number is given by $N_{Sc} = \nu/D$ and, since D is generally much smaller than κ in liquids and solids, N_{Sc} is usually much larger than N_{Pr}. This means that the thickness of the mass transfer boundary layer will be much smaller than the thermal transfer boundary layer. Even when thermal transfer occurs through a turbulent boundary layer, mass transfer may still occur through the laminar sublayer and the above equations remain applicable.

The ratio between the rates of heat and mass transfer is given by:

$$\frac{\dot{M}}{\dot{Q}} = \frac{(C_b - C_f)}{(T_b - T_f)}\frac{1}{\rho c_P}\left(\frac{D}{\kappa}\right)^{2/3} \tag{13}$$

Because the ratio D/κ is typically about 1/1000, the diffusion time is about 100 times longer than the thermal cooling time. For this reason, a magma ocean freezes long before much material exchange with an underlying molten iron layer can occur, as discussed further below: it is a simple consequence of the relative magnitudes of the material and thermal diffusion coefficients.

Chemical equilibration is much faster when the diffusive exchange takes place between the magma ocean and small falling metal droplets ('metal rain'). In this case the large surface area of the droplets more than compensates for the small material diffusion coefficient (of course, the droplet still equilibrates thermally much faster than it does chemically). For a small metal droplet of diameter d with an exchange surface area given approximately by $\pi(d/2)^2$, the rate of mass transfer $\dot{M}$ implies that the mass concentration in the metal droplet C_m changes as:

$$\frac{[C_m(t) - C_s(t)]}{[C_m(0) - C_s(0)]} = \exp\left\{-0.996\,\frac{D^{2/3}v_s^{1/2}}{d^{3/2}\nu^{1/6}}t\right\} \tag{14}$$

where C_s is the concentration in the silicate magma ocean and v_s is the terminal settling velocity of the droplet (subsequently referred to as the 'settling velocity'). During the time required for the droplet to achieve 99% equilibration with the magma ocean, it falls a distance:

$$z_{\text{equilib}} = 4.624\,\frac{d^{3/2}\nu^{1/6}v_s^{1/2}}{D^{2/3}} \tag{15}$$

With a viscosity $\eta = 10^{-2}$ Pa s and a diffusion coefficient $D = 10^{-8}\ m^2\ s^{-1}$, the mean droplet diameter is $\sim$1 cm and the settling velocity is $\sim$0.5 $m\ s^{-1}$ (see below). These values give an equilibration distance of $\sim$60 m, which is negligible compared with the depth of the magma ocean itself. Under these conditions the Reynolds number Re_L

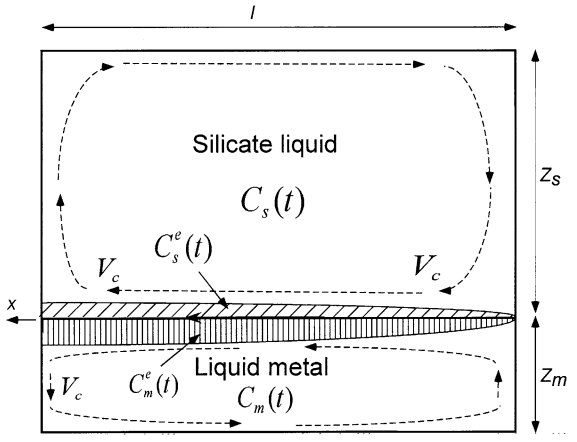

Fig. 3. Details of the metal layer model. A silicate liquid magma ocean, of depth Z_s, overlies a layer of liquid metal of depth Z_m. The convection cells in the two layers are assumed to be coupled, the convection velocity is v_c, and the width of the cells is l. The shaded regions show the volumes of silicate and metal that have equilibrated by diffusion across the interface; at time t, the respective equilibrated compositions are $C_s^e(t)$ and $C_m^e(t)$ and the bulk compositions of the silicate and metal layers are $C_s(t)$ and $C_m(t)$, respectively.

is about 2000, so that the approximations used here should be quite accurate.

4. Metal layer equilibration model

4.1. Model setup

This model is based on the concept that liquid metal settles rapidly out of the magma ocean and ponds temporarily at its base immediately above crystalline or partially crystalline lower mantle (Figs. 1 and 3). Equilibration of silicate liquid with the underlying metal layer involves chemical diffusion of siderophile elements through the conductive boundary layer that is present at the base of the vigorously convecting magma ocean ([3], Fig. 1). Diffusion through this boundary layer controls the equilibration rate up to ~25 GPa because diffusion rates are slower in liquid silicate than in liquid metal up to this pressure at relevant temperatures (Fig. 2). At significantly higher pressures, diffusion through a boundary layer at the top of the metal layer could become rate-controlling. In order to consider metal–silicate equilibration rates that depend on diffusion in either silicate or in metal, we develop the model shown in Fig. 3. For convenience, we assume that the convective velocity v_c is the same in both the silicate magma ocean and underlying metal layer and that the widths of the respective convection cells are also the same. These assumptions will be valid if convection in the two layers is strongly coupled. However, the assumptions are not critical for the results because equilibration will still be controlled by diffusion through the respective boundary layers whether convection is coupled or not.

Consider the metal and silicate boundary layers flowing at velocity v_c along the metal–silicate interface in convection cells of width l (Fig. 3). After a time interval x/v_c, the equilibration distances in silicate and metal are approximately $\sqrt{D_{S,s}x/v_c}$ and $\sqrt{D_{S,m}x/v_c}$, respectively, where $D_{S,s}$ and $D_{S,m}$ are diffusion coefficients for siderophile elements in silicate and metal respectively. The mass of silicate that equilibrates in time $\delta t = l/v_c$ is then given by $\rho_s \int_0^l \sqrt{D_{S,s}x/v_c}\,dx = (2/3)\rho_s\sqrt{D_{S,s}l^3/v_c}$ and, similarly, the mass of equilibrated metal is $(2/3)\rho_m\sqrt{D_{S,m}l^3/v_c}$, where ρ_s and ρ_m are the respective silicate and metal densities. We now define several relevant mass fractions:

1. Mass fractions of metal and silicate in the entire magma ocean–metal layer system are assumed to be identical to the current mass fractions of the mantle and core and are defined as:

$$\Phi_m = z_m\rho_m/(z_m\rho_m + z_s\rho_s) = 0.32 \quad (16)$$

$$\Phi_s = 1-\Phi_m = 0.68 \quad (17)$$

2. Based on definitions given above, the respective mass fractions of metal and silicate that equilibrate in time δt (shaded regions in Fig. 3) are given by:

$$f_m^{ms} = \rho_m\sqrt{D_{S,m}}/\left(\rho_m\sqrt{D_{S,m}} + \rho_s\sqrt{D_{S,s}}\right) \quad (18)$$

and

$$f_s^{ms} = 1-f_m^{ms} \quad (19)$$

3. The mass fraction of metal that equilibrates in time δt, relative to the entire metal layer, is:

$$f_m^m = \frac{(2/3)\sqrt{D_{S,m} l^3 / v_c}}{z_m l} \quad (20)$$

where z_m is the depth of the metal layer.

From mass balance, the composition of equilibrated metal at time t is given by:

$$C_m^e(t) = \frac{C_B^e(t)}{f_m^{ms} + f_s^{ms}/D^{ms}} \quad (21)$$

where D^{ms} is the metal–silicate distribution coefficient, and $C_B^e(t)$ is the bulk composition of the equilibrated regions, which is given by:

$$C_B^e(t) = f_m^{ms} C_m(t) + f_s^{ms} C_s(t) \quad (22)$$

where $C_m(t)$ and $C_s(t)$ are the bulk metal and silicate compositions at time t. The silicate composition can be eliminated from this expression using definitions of the bulk composition C_B of the magma ocean–metal system:

$$C_B = \Phi_m C_m(0) + \Phi_s C_s(0) = \Phi_m C_m(t) + \Phi_s C_s(t) \quad (23)$$

where $C_m(0)$ and $C_s(0)$ are the original metal and silicate bulk compositions, from which:

$$C_s(t) = (\Phi_m/\Phi_s)(C_m(0) - C_m(t)) + C_s(0). \quad (24)$$

Substituting Eqs. 22 and 24 into Eq. 21 gives:

$$C_m^e(t) = \frac{C_m(t)(\Phi_s f_m^{ms} - \Phi_m f_s^{ms}) + f_s^{ms}(\Phi_m C_m(0) + \Phi_s C_s(0))}{\Phi_s (f_m^{ms} + f_s^{ms}/D^{ms})} \quad (25)$$

We assume that the magma ocean and metal layer each homogenize rapidly, because of turbulent convection, once material in the conductive boundary layers is transported away from the metal–silicate interface. The homogenized metal composition at time $(t+\delta t)$ is then:

$$C_m(t + \delta t) = (1 - f_m^m) C_m(t) + f_m^m C_m^e(t) \quad (26)$$

The rate of change of metal composition is:

$$\frac{dC_m}{dt} = \frac{C_m(t - \delta t) - C_m(t)}{\delta t} \quad (27)$$

and on substituting Eqs. 25 and 26 and $\delta t = l/v_c$ we obtain:

$$\frac{dC_m}{dt} = aC_m(t) + b \quad (28)$$

where

$$a = \frac{f_m^m v_c}{l}\left[\frac{\Phi_s f_m^{ms} - \Phi_m f_s^{ms}}{\Phi\ (f_m^{ms} + f_s^{ms}/D^{ms})} - 1\right]$$

and

$$b = \frac{f_m^m v_c}{l}\left[\frac{f_s^{ms}\ (\Phi_m C_m(0) + \Phi_s C_s(0))}{\Phi_s\ (f_m^{ms} + f_s^{ms}/D^{ms})}\right]$$

Finally, with $C_m = C_m(0)$ at $t = 0$, where $C_m(0)$ is the initial metal composition:

$$C_m(t) = \left[\left(C_m(0) + \frac{b}{a}\right)\exp(at)\right] - \frac{b}{a} \quad (29)$$

Note that the metal composition after complete equilibration is given by $C_m^{eq} = b/a$.

In the case that diffusion and convection are orders of magnitude faster in the metal than in the silicate, so that the metal homogenizes rapidly on the time scale δt, $f_m^m = 1$ and, in place of Eq. 18, $f_m^{ms} = z_m l \rho_m / (z_m l \rho_m + (2/3)\rho_s \sqrt{D_{S,s} l^3 / v_c})$.

4.2. Results

We have calculated equilibration times for the metal layer model as a function of magma ocean depth using Eq. 29 and parameters derived either above or listed in Table 1. We use typical low-pressure concentration values for Ni as the starting compositions ($C_m(0)$ and $C_s(0)$) based on metal and silicate compositions in a small planetesimal such as asteroid 4 Vesta [25]. Using a

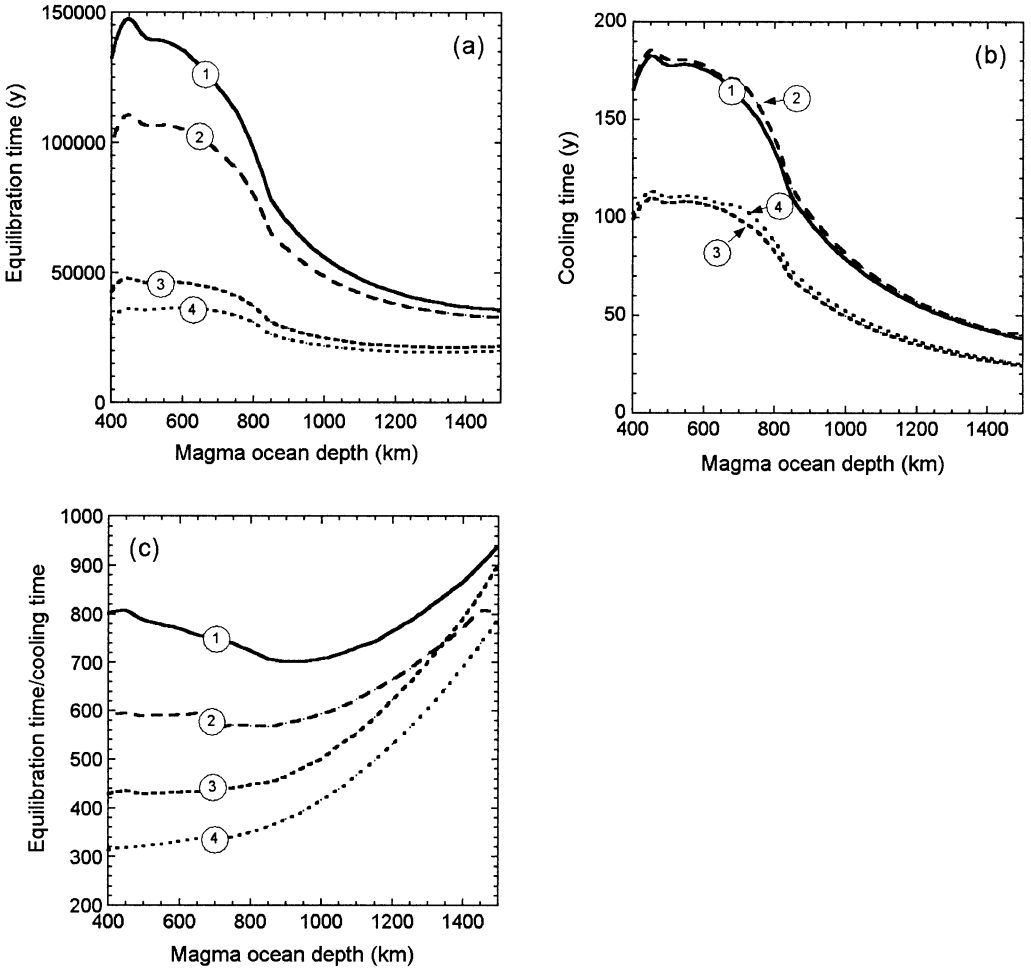

Fig. 4. Results of the metal layer model for magma oceans with depths ranging from 400 to 1500 km. Equilibration times (a), cooling times (b), and the ratio of equilibration times to cooling times (c) are shown as a function of magma ocean depth. Results obtained using parameters listed in Table 1 and the text are shown by solid lines, labeled (1), and the dashed lines show the effects of varying some key parameters. Curves labeled (2) show the effect of increasing the temperature at the base of the magma ocean to 100 K above the liquidus; (3) shows the effect of reducing the silicate liquid viscosity by a factor of 10; (4) shows the combined effects of higher temperature and lower viscosity.

metal–silicate distribution coefficient that is consistent with the current Ni content of the terrestrial mantle (Table 1), we calculate the time for the metal composition to reach 99% of its equilibrium value, i.e. $(C_m(0)-C_m(t))/(C_m(0)-C_m^{eq}) = 0.99$. The time for cooling to reduce the temperature at the metal–silicate interface to 200 K below the liquidus by radiative heat loss is also determined as described above. We present results for magma oceans with depths up to 1500 km to also test the possibility that the concentrations of siderophile elements in the mantle resulted from *partial* equilibration at the base of a magma ocean significantly deeper than 800 km.

Results are presented in Fig. 4. For magma oceans with depths ranging from 400 to 1500 km, the Rayleigh number varies from 10^{28} to 10^{32}, average viscosities from 10^{-2} to 3×10^{-5} Pa s, and convection velocities from 3.3 to 11.6 m s^{-1}. Calculated equilibration times for magma

oceans with depths of 400–1500 km, using parameters described above, lie in the range 4×10^4 to 1.5×10^5 yr (Fig. 4a). In contrast, cooling times lie in the range 40–165 yr and are two to three orders of magnitude shorter than equilibration times (Fig. 4b,c). Note that the cooling times are similar to previous estimates [11,26]. The complex trends shown in Fig. 4 result from the combined effects of increasing depth (which increases both the volume of materials that have to equilibrate and the Rayleigh number), increasing temperature, the non-linear topology of the peridotite liquidus, and the effects of P and T on the transport properties of metal and silicate (Fig. 2).

Equilibration times can be shortened significantly by changing some input parameters. For example, increasing the temperature at the base of the magma ocean by 100 K reduces equilibration times by up to 20% whereas cooling times are hardly affected (Fig. 4, curves 2). (Note that an overstep of 100 K may be unrealistically high because the silicate mantle underlying the metal layer must be largely crystalline in order to physically support the liquid metal layer; see Fig. 1.) Decreasing the silicate melt viscosity by an order of magnitude can reduce equilibration times by a factor of up to 3 and cooling times by a factor of 1.5 (Fig. 4, curves 3). Fig. 4 shows the combined effects of these changes (curves 4) – note that equilibration times are still larger than cooling times by a factor of 300–800. It should also be noted that calculated equilibration times are based on constant temperature and will therefore be underestimates.

The effects on the results of the approximations that we have made are small. For example, the results are insensitive to the density values used for metal and silicate. In reality, these will vary with depth in the magma ocean and the fixed values used (Table 1) are only broad approximations. Changing the values to 7000 and 3000 kg m^{-3} for metal and silicate respectively, for example, changes the equilibration and cooling times by $<3\%$ and the ratio of these times by $\sim1\%$. The large uncertainty in peridotite liquidus temperatures above 25 GPa also has a minor effect on the conclusions. Reducing the liquidus temperature by 800 K at 1500 km depth, from ~4700 to ~3900 K (cf. [18,19]), increases the equilibration time by a factor of 2.3, the cooling time by a factor of 2.1, but their ratio by $<10\%$.

In the case that the magma ocean is partially crystalline, rather than completely molten as assumed here, viscosities will be higher and diffusivities slower. The expression for the effective viscosity of partially crystalline magma, $\eta_{\rm eff}=\eta\exp(23.03\phi)$ where η is the silicate liquid viscosity and ϕ is the average fraction of crystals present [3], predicts a viscosity increase of an order of magnitude for each incremental increase of ϕ of 0.1. In contrast, the effective diffusivity is likely to change by less than an order of magnitude for $\phi<0.5$ [27]. With 30% crystallization, assuming that the viscosity is increased by a factor of 10^3 and diffusivity is unchanged relative to the completely molten state, the ratio of equilibration time to cooling time is still in excess of two orders of magnitude.

5. Metal droplet equilibration model

The separation of metal from silicate in a magma ocean occurs by the settling of liquid metal droplets, i.e. by 'metal rainfall' [1]. Here we develop simple kinetic models to determine if metal–silicate equilibration is maintained as metal droplets sink. Equilibration times depend critically on the diameter of the metal droplets [12] and we estimate stable droplet sizes using fluid dynamics.

5.1. Model setup

Consider a single spherical metal droplet, of radius r, settling through silicate liquid with settling velocity v_s. Reaction between metal and silicate occurs in the time, $\delta t=2r/v_s$, that it takes the droplet to fall a distance equal to its own diameter (Fig. 5). Even though diffusion in metal may be as slow as in silicate liquid (Fig. 2), we assume in the following derivation that the metal droplets develop an internal circulation that rapidly homogenizes their composition. In this case, equilibration of the silicate liquid occurs to a distance $\delta x\approx\sqrt{2D_Sr/v_s}$ by diffusion through a boundary layer. The mass of silicate that equili-

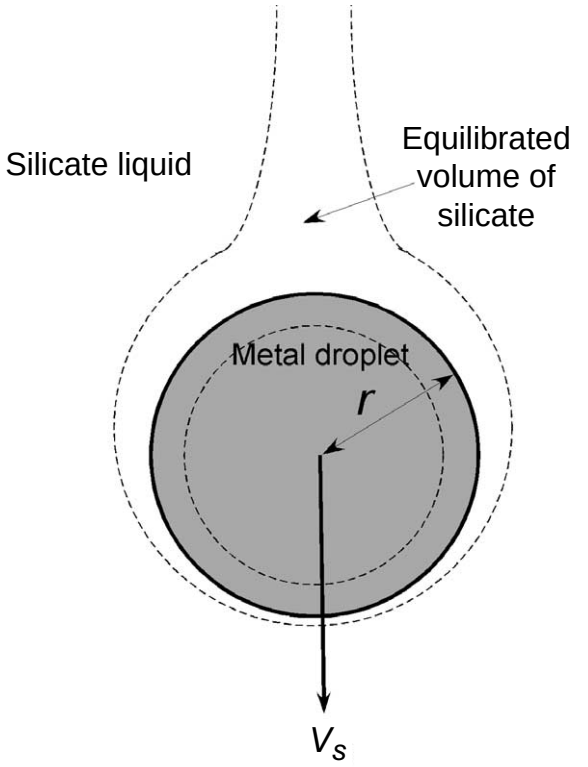

Fig. 5. Metal droplet model: a spherical droplet of liquid metal, of radius r, sinks through silicate liquid with terminal settling velocity v_s. The volumes of metal and silicate that equilibrate are shown schematically by dashed lines.

brates in time δt is $\sim 4\pi r^2 \rho_s \sqrt{2D_S r/v_s}$ and the mass of equilibrated metal is $4\pi r^3 \rho_m/3$. Thus the mass fractions of the equilibrated metal and silicate components are, respectively:

$$F_m = \frac{r^3 \rho_m/3}{r^3 \rho_m/3 + r^2 \rho_s \sqrt{2D_S r/v_s}} \tag{30}$$

and

$$F_s = 1 - F_m. \tag{31}$$

Following the previous derivation, the composition of the metal at time $t+\delta t$ is:

$$C_m(t+\delta t) = \frac{C_B(t)}{F_m + F_s/D^{ms}} \tag{32}$$

and the bulk composition of the equilibrated components is:

$$C_B(t) = F_m C_m(t) + F_s C_s(0) \tag{33}$$

where $C_s(0)$ is the original silicate composition – which is applicable in the case of a single falling metal droplet. The rate of change of the metal composition is:

$$\frac{dC_m}{dt} = [C_m(t+\delta t) - C_m(t)]/\delta t =$$

$$\frac{v_s}{2r}\left[\frac{F_m C_m(t) + F_s C_s(0)}{F_m + F_s/D^{ms}} - C_m(t)\right] \tag{34}$$

which gives:

$$\frac{dC_m}{dt} = A C_m(t) + B \tag{35}$$

where:

$$A = \frac{v_s}{2r}\left[\frac{F_m}{F_m + F_s/D^{ms}} - 1\right]$$

and

$$B = \frac{v_s}{2r}\left[\frac{F_s C_s(0)}{F_m + F_s/D^{ms}}\right]$$

Finally, integrating with $C_m = C_m(0)$ at $t = 0$ gives:

$$C_m(t) = \left[\left(C_m(0) + \frac{B}{A}\right)\exp(At)\right] - \frac{B}{A} \tag{36}$$

which is identical in form to Eq. 29.

We have also used a finite difference model to check the results obtained using Eq. 36. The one-dimensional diffusion equation (spherical coordinates) is solved using a Crank–Nicholson approximation. As above, we consider diffusion in the silicate liquid to be rate-limiting. In this case, the composition of the silicate adjacent to the droplet is reset to $C_s(0)$ at time intervals equivalent to the time taken for the droplet to fall a distance equal to its own diameter. The change in metal composition is calculated from the flux at the interface using Fick's first law and the equilibrium silicate composition at the interface is determined from D^{ms}.

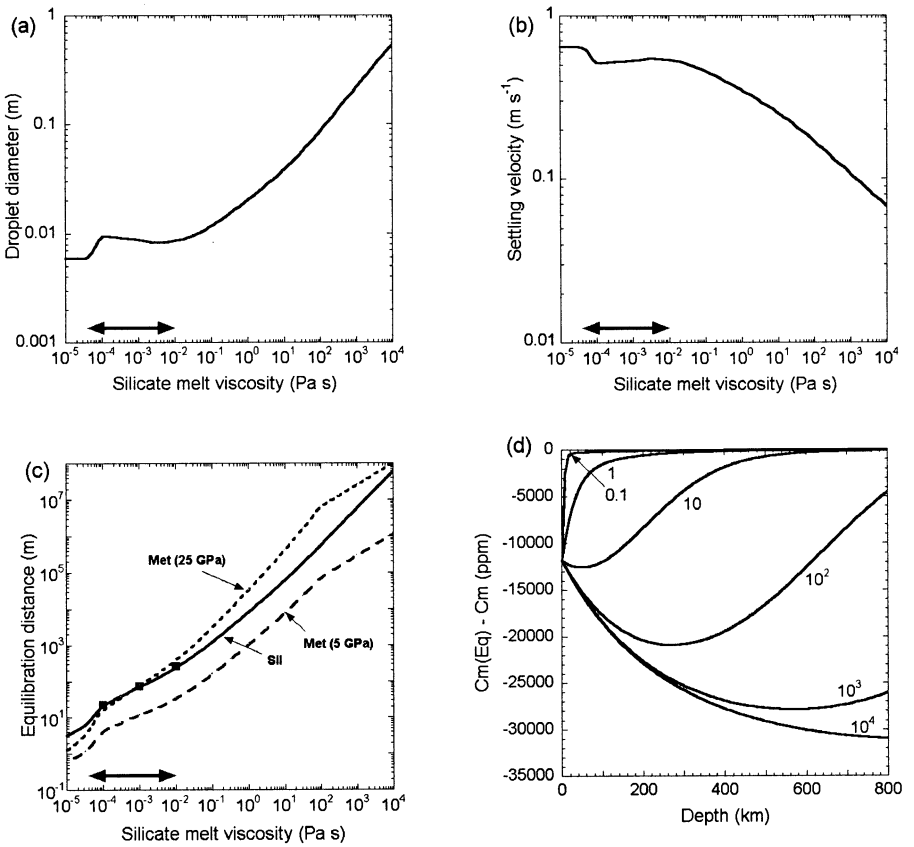

Fig. 6. Results of metal droplet models. Results in panels a–c are shown as a function of silicate melt viscosity; the arrowed lines show the likely viscosity range for magma oceans with depths in the range 400–1500 km. (a) Stable droplet diameter, calculated for the Weber number = 10. (b) Terminal settling velocity of a droplet. (c) Equilibration distance for a single metal droplet: the solid line ('Sil') shows the results obtained using Eq. 36 and the three square symbols show results of the finite difference model, both cases being based on the assumption that equilibration is controlled by diffusion in silicate liquid. The broken lines ('Met') show estimates at 5 and 25 GPa calculated from Eq. 37 assuming that diffusion in the metal droplet controls the equilibration rate. (d) The difference between the equilibrium metal composition (Cm(Eq)) and the composition (Cm) of a single droplet as a function of settling distance in a magma ocean 800 km deep. The metal–silicate distribution coefficient varies from ~500 close to the surface to ~28 at a depth of 800 km according to [32]. Results are shown and labeled for silicate liquid viscosities in the range 10^{-1} to 10^{4} Pa s.

Finally, we consider the case where diffusion in the metal droplet controls the equilibration rate due to an absence of internal circulation in the droplet. In this case, the metal composition at the interface is fixed at $C_s(0)D^{ms}$ and the average composition of the metal, C_m^{av}, is determined as a function of time from [27]:

$$\frac{C_m(0)-C_m^{av}(t)}{C_m(0)-C_s(0)D^{ms}} = 1-\frac{6}{\pi^2}\sum_{n=1}^{\infty}\frac{1}{n^2}\exp(-D_{S,m}n^2\pi^2 t/r^2) \quad (37)$$

5.2. Settling velocity of iron droplets

We computed the terminal settling velocity of iron droplets by assuming that they are smooth, rigid spheres. In fact, as the droplets fall, they become flattened into lentil-like shapes that fall at velocities different from those of rigid spheres [28], but this effect is small compared to other uncertainties in this problem and we neglect it here. We follow a procedure due to [29]. We first compute a dimensionless friction coefficient:

$$f = \frac{\pi}{6}\left(\frac{\rho_m - \rho_s}{\rho_s}\right)\left(\frac{\rho_s}{\eta}\right)^2 g d^3 \quad (38)$$

where g is the acceleration of gravity, η is the viscosity of the silicate melt and d is the diameter of the droplet. When f is less than 10, the droplet is in the laminar flow regime and its settling velocity v_s is computed from Stoke's law:

$$v_s = \frac{(\rho_m - \rho_s) g d^2}{18\eta} \quad (39)$$

If f is greater than 10, a polynomial fit to the drag coefficient C_D for a sphere, as a function of the friction coefficient, is used, based on data in [29] (figure 125). The settling velocity is then given by:

$$v_s = \sqrt{\frac{4}{3C_D}\left(\frac{\rho_m - \rho_s}{\rho_s}\right) g d} \quad (40)$$

At very high values of the friction factor, the drag coefficient is set to an asymptotic value of 0.2. The drag coefficient has a well-known minimum (due to the 'drag crisis' at which the boundary layer transforms from laminar to turbulent) in the vicinity of $f = 10^{10}$. This transformation results in a non-linear trend for low viscosities (Fig. 6).

5.3. The size of falling droplets

When any mass of dense liquid falls through a less dense liquid, instabilities tend to form at the interface that may eventually disperse the dense mass. These include both Rayleigh–Taylor instabilities that arise from the density differences alone and Kelvin–Helmholtz instabilities that arise from velocity gradients across the surface [30]. It can easily be shown that the lowest Rayleigh–Taylor, 'pancake' flattening mode of a dense, falling sphere spreads it to twice the original diameter after it falls only a few times its own diameter. This disruption distance is particularly short for a fluid sphere falling through another fluid of comparable density. The distance contains a factor of $\sqrt{\rho_m/\rho_s d}$, so that a dense mass falling through a very low-density atmosphere would remain intact much longer than a dense mass falling through a magma ocean of similar density. As further, smaller-scale instabilities disrupt the falling mass, the sizes of liquid iron masses decrease until further disruption is halted by the surface energy of the droplets.

Surface tension tends to draw the drops together into spherical droplets that resist further breakup because new surface area must be created [31]. Both experiments and theoretical studies show that a dimensionless number, the ratio between the stagnation pressure and the internal pressure caused by surface tension, determines the point at which falling liquid droplets become stable. This number is called the Weber number and is given by:

$$We = \frac{(\rho_m - \rho_s) d\ v_s^2}{\sigma} \quad (41)$$

where σ is the surface energy of the metal–silicate interface. Falling droplets are stable against disruption when the value of We falls to about 10. Larger values imply instability. We have used this criterion to determine the stable size of falling metal droplets as shown in Fig. 6a. We then use the stable size to evaluate the rate at which such falling droplets chemically equilibrate with the surrounding silicate liquid.

A question that often arises is: how quickly does a falling blob of a given size break up into droplets of the size given by the Weber number? As the Earth accreted, planetesimals with cores impacting the surface may have delivered iron in blobs of perhaps 50 to even 500 km in diameter. Can such blobs really break up into a rain of small iron droplets? In the later stages of Earth accretion, the impact velocity is of the order of the escape velocity, perhaps 10 km s^{-1}. In this case, the iron is already dispersed on impact: it is strongly sheared and thinned for oblique impacts, but even in near-vertical impacts it lines the crater as it expands and may thus quickly decease its thickness by a factor of two or more during a penetration of a few times its own diameter. Later, in a magma ocean stage, the Rayleigh–Taylor instabilities described above reduce it further. It is easy to show that these instabilities initiate a cascade of disruption that quickly re-

duces the droplet size to its stable value. If the diameter, d, of the initial blob is halved in its initial fall through the characteristic distance $l=\sqrt{\rho_m/\rho_s d}$, then the first generation of daughter blobs are halved after falling a distance of $l/2$. The second generation divides after a distance of $l/4$. In general, the mth generation has formed after falling a distance of $l/2^m$. The total distance to divide from d to a final size of $d/2^m$ is thus the series $(1+1/2+1/2^2...1/2^m)l \rightarrow 2l$ as $m \rightarrow \infty$. Thus, unless the initial cores impacting the top of the magma ocean have diameters approaching the depth of the magma ocean itself, they will quickly break up into a shower of small droplets that cascade through the magma ocean.

5.4. Results

The stable size and settling velocity of metal droplets as a function of magma ocean viscosity are shown in Fig. 6a,b. For magma oceans of depths in the range 400–1500 km, the average silicate liquid viscosity is predicted to lie in the range 10^{-2} to 3×10^{-5} Pa s. Over this viscosity range, the droplet size and settling velocity are almost constant. The stable droplet diameter is predicted to be 0.8–1.1 cm (which is similar to the maximum size estimated by [1,12]) and the settling velocity 0.46–0.55 m s^{-1} (Fig. 6a,b). Using these results, we have calculated equilibration times from the metal droplet models as a function of magma ocean viscosity using Eq. 36 and parameters either derived above or listed in Table 1. Using typical low-pressure concentration values for Ni as the starting compositions ($C_m(0)$ and $C_s(0)$) and a metal–silicate distribution coefficient that is consistent with the current Ni content of the mantle (Table 1), we calculate the time for the metal droplet composition to reach 99% of its equilibrium value, i.e. $(C_m(0)-C_m(t))/(C_m(0)-C_m{}^{eq})=0.99$. The results, shown in Fig. 6c, indicate that equilibration will be attained after a settling distance of 6–250 m over the viscosity range of interest if equilibration is controlled by diffusion in the silicate liquid. The results obtained using Eq. 36 and the finite difference model (described above) differ by less than 4% (Fig. 6c). Equilibration distances predicted using Eq. 15 also agree within an order of magnitude over the viscosity range of interest. If equilibration is controlled by diffusion in the metal (Eq. 37), equilibration distances depend on pressure but are still very small compared with magma ocean depths. At the base of a magma ocean 700 km deep, the equilibration distance at 25 GPa and a viscosity of 2×10^{-3} Pa s is less than 200 m according to Eq. 37.

We have studied the extent to which equilibrium is maintained as a single metal droplet sinks in a magma ocean 800 km deep using a polybaric equilibration model for Ni partitioning. The magma ocean is divided into small depth increments (10 m thick) and the metal–silicate partition coefficient varies with P, T and fO_2 (according to formulations of [32]). Initial compositions are listed in Table 1. Eq. 36 is used to calculate the new droplet composition in each successive depth increment. In this model, D^{ms} varies from $\sim$500 near the surface to 28 at the base of the magma ocean. Results are plotted in Fig. 6d as the difference between the droplet composition and the equilibrium metal composition as a function of settling depth for a range of silicate viscosities (using droplet sizes and settling velocities as shown in Fig. 6a,b). For silicate viscosities ≤ 0.1 Pa s (applicable to a magma ocean 800 km deep), droplets equilibrate rapidly and equilibrium is maintained as they sink. For higher viscosities (e.g. 1–10 Pa s), disequilibrium is maintained for at least a significant part of the 800 km settling distance. For viscosities ≥ 100 Pa s, equilibrium is never achieved and when the viscosity is $\geq 10^4$ Pa s, the droplets effectively preserve their original composition all the way to the base of the magma ocean.

6. Implications for magma ocean depth

Metal–silicate partition coefficients for a number of the moderately siderophile elements reach values that are consistent with core–mantle concentrations at certain conditions of high P and T [6–8,25,32]. In the case of the (unrealistic) metal layer model, these conditions would correlate with the base of the magma ocean and would therefore

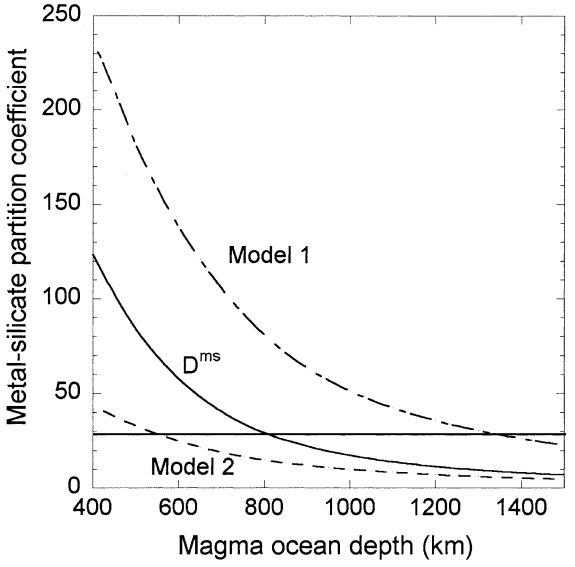

Fig. 7. Results of equilibrium metal–silicate fractionation models. D^{ms} is the metal–silicate partition coefficient for Ni at the base of the magma ocean, calculated as a function of magma ocean depth from [32]. The two dashed lines show the results of the fractionation models discussed in the text and show the effective partition coefficient (Ni concentration in metal/Ni concentration in silicate) after metal–silicate segregation is complete. The horizontal line indicates the core–mantle Ni partition coefficient value of ~28.

indicate its depth. However, in the case of the metal droplet model, the interpretation of apparent pressures and temperatures of equilibration is more complex, as discussed recently by Li and Agee [7]. It is clear from the above results that the final equilibration between metal droplets and silicate liquid will take place at the base of the magma ocean immediately prior to segregation. However, because of fractionation effects, the resulting siderophile element contents of the core and mantle are unlikely to record the distribution coefficients at that depth. We demonstrate this point through two simple end-member equilibrium metal–silicate fractionation models. The starting point for both models is a magma ocean that contains uniformly dispersed metal droplets. We calculate a magma ocean adiabat (see Section 2) and metal–silicate distribution coefficients for Ni, D^{ms}_{Ni}, as a function of depth from [32]. Oxygen fugacity and other variables are adjusted to give $D^{ms}_{Ni} = 28$ (as required for core–mantle equilibration) at a depth of ~800 km (Fig. 7).

6.1. Fractionation model 1

In the first model we assume that metal droplets sink and segregate on a time scale that is very rapid compared with the time scale of convective flow and mixing of the magma ocean. The magma ocean is divided into n depth increments, each initially consisting of 32 wt% metal and 68 wt% silicate liquid (i.e. core–mantle proportions). Assuming an initially chondritic bulk composition, the equilibrium metal composition in each depth increment is calculated from:

$$C_m(i) = \frac{C_B(i)}{0.32 + 0.68/D^{ms}_{Ni}(i)} \quad (42)$$

where $C_B(i)$ is the bulk composition of the ith depth increment. After calculating the metal composition in each increment, the metal is moved down by one depth increment and new values of $C_B(i)$, $C_m(i)$ and the corresponding silicate composition ($C_S(i)$) are calculated. This procedure is repeated until all metal has segregated at the base of the magma ocean. The final bulk composition of the segregated metal and the average composition of the remaining silicate magma are calculated and a core–mantle partition coefficient is thus obtained. The results (with $n = 500$) show that a magma ocean with a depth of ~1350 km (i.e. much deeper than 800 km) is required to give a core–mantle partition coefficient of 28 for Ni (Fig. 7). This is because metal–silicate equilibration at low pressures contributes significantly to the final composition of the silicate (and consequently also to that of the metal). This model is only fully realistic if the metal sinks and segregates very rapidly because it is assumed that there is no mixing or convective transport of the silicate magma.

6.2. Fractionation model 2

In this model, we assume that vigorous convection keeps the silicate magma ocean fully mixed and chemically homogeneous and that metal

droplets are suspended in the magma ocean and only segregate gradually as they enter the boundary layer at its base [3]. The segregation of metal fractions that equilibrate finally with silicate at the base of the magma ocean cause the bulk composition of the magma ocean, the mass fraction of remaining dispersed metal and thus the composition of the segregating metal to change continuously. A numerical simulation of this fractionation process shows that a magma ocean depth of ~550 km results in a core–mantle partition coefficient of 28 (Fig. 7).

From the results of Fig. 7, it is clear that the compositions of metal and silicate that result from the segregation of metal droplets in a magma ocean depend strongly on the dynamics of segregation, convection and chemical mixing. In reality, metal–silicate fractionation is likely to involve processes intermediate between those of the end-member models 1 and 2. However, a more detailed analysis will be required to obtain a definitive solution to this problem.

7. Conclusions

The results presented above show conclusively that liquid metal of the proto-core could not have equilibrated chemically as a layer at the base of a deep magma ocean because the required equilibration times are two to three orders of magnitude greater than magma ocean cooling times. Once such a layer has formed, it is chemically isolated from the overlying magma ocean and cannot even partially equilibrate before the onset of crystallization. Note that the lifetime of the magma ocean cannot be extended significantly by the energy of continuing impacts because the necessary accretion rate would have to be unrealistically high [26]. Furthermore, the liquid metal layer at the base of the magma ocean is gravitationally highly unstable and its lifetime is severely limited by the time scale at which Rayleigh–Taylor instabilities develop and cause the metal to descend further as diapirs [1,12] (see Fig. 1).

In contrast, small metal droplets equilibrate rapidly with silicate liquid as they sink through the magma ocean, as previously concluded by [1,12]. For all reasonable models and parameter sets, equilibration is maintained when droplets sink and partition coefficients change as P and T increase. Thus, the only way that a high-pressure siderophile element signature could have been imparted on the mantle in a magma ocean was by 'metal rainfall' involving chemical equilibration between small (~1 cm) settling metal droplets and silicate liquid (see also [12]). If the Earth had accreted largely from planetesimals that already contained existing metallic cores, the metal could only have equilibrated with silicate liquid in a magma ocean if the metal melted and became finely dispersed as small droplets. Chemical interaction between metal droplets and silicate liquid can be investigated using polybaric fractionation models. Preliminary results show that the depth of the magma ocean may differ significantly from the depth suggested by the apparent equilibration pressure.

Acknowledgements

Mike Drake is acknowledged for generously supporting two visits to the LPL by D.C.R. Grant NAG5-9435 to M.J. Drake and the German Science Foundation Priority Program on 'Silicate Melts' (Grants Ru 437/5-1 and Ru 437/5-2) funded part of this work. We thank Y. Abe for valuable discussions and Dave Stevenson and Michael Walter for helpful and constructive reviews. *[BW]*

References

[1] D.J. Stevenson, Fluid dynamics of core formation, in: H. Newsom, J.H. Jones (Eds.), The Origin of the Earth, Oxford Press, London, 1990, pp. 231–249.
[2] G.F. Davies, Heat deposition and retention in a solid planet growing by impacts, Icarus 63 (1985) 45–68.
[3] W.B. Tonks, H.J. Melosh, The physics of crystal settling and suspension in a turbulent magma ocean, in: H. Newsom, J.H. Jones (Eds.), The Origin of the Earth, Oxford Press, London, 1990, pp. 151–174.
[4] A.E. Ringwood, Chemical evolution of the terrestrial planets, Geochim. Cosmochim. Acta 30 (1966) 41–104.
[5] C.J. Capobianco, J.H. Jones, M.J. Drake, Metal-silicate thermochemistry at high temperature: magma oceans and

the 'excess siderophile element' problem of the Earth's upper mantle, J. Geophys. Res. 98 (1993) 5433–5443.
[6] J. Li, C.B. Agee, Geochemistry of mantle-core formation at high pressure, Nature 381 (1996) 686–689.
[7] J. Li, C.B. Agee, The effect of pressure, temperature, oxygen fugacity and composition on partitioning of nickel and cobalt between liquid Fe-Ni-S alloy and liquid silicate: implications for the Earth's core formation, Geochim. Cosmochim. Acta 65 (2001) 1821–1832.
[8] K. Righter, M.J. Drake, G. Yaxley, Prediction of siderophile element metal/silicate partition coefficients to 20 GPa and 2800°C: the effects of pressure, temperature, oxygen fugacity, and silicate and metallic melt compositions, Phys. Earth Planet. Int. 100 (1997) 115–134.
[9] E. Ohtani, H. Yurimoto, S. Seto, Element partitioning between metallic liquid, silicate liquid, and lower mantle minerals: implications for core formation of the Earth, Phys. Earth Planet. Int. 100 (1997) 97–114.
[10] E. Ito, T. Katsura, T. Suzuki, Metal/silicate partitioning of Mn, Co, and Ni at high pressures and high temperatures and implications for core formation in a deep magma ocean, in: M.H. Manghnani (Ed.), Properties of Earth and Planetary Materials at High Pressure and Temperature, Geophysical Monograph 101, AGU, Washington, DC, 1998, pp. 215–225.
[11] V.S. Solomatov, Fluid dynamics of a terrestrial magma ocean, in: R.M. Canup, K. Righter (Eds.), Origin of the Earth and Moon, Univ. of Arizona Press, Tucson, AZ, 2000, pp. 323–338.
[12] S.-I. Karato, V.R. Murthy, Core formation and chemical equilibrium in the Earth-I. Physical considerations, Phys. Earth Planet. Int. 100 (1997) 61–79.
[13] T. Rushmer, W.G. Minarik, G.J. Taylor, Physical processes of core formation, in: R.M. Canup, K. Righter (Eds.), Origin of the Earth and Moon, Univ. of Arizona Press, Tucson, AZ, 2000, pp. 227–243.
[14] J.J. Niemela, L. Skrbek, K.R. Sreenivasan, R.J. Donnelly, Turbulent convection at very high Rayleigh numbers, Nature 404 (2000) 837–840.
[15] J.F. Kasting, Runaway and moist greenhouse atmospheres and the evolution of Earth and Venus, Icarus 74 (1988) 472–494.
[16] K. Zahnle, J.F. Kasting, J.B. Pollack, Evolution of a steam atmosphere during Earth's accretion, Icarus 74 (1988) 62–97.
[17] C. Herzberg, J. Zhang, Melting experiments on anhydrous peridotite KLB-1: compositions of magmas in the upper mantle and transition zone, J. Geophys. Res. 101 (1996) 8271–8295.
[18] E. Ohtani, Melting temperature distribution and fractionation in the lower mantle, Phys. Earth Planet. Int. 33 (1983) 12–25.
[19] R. Boehler, Melting temperature of the Earth's mantle and core: Earth's thermal structure, Annu. Rev. Earth Planet. Sci. 24 (2000) 15–40.
[20] G.H. Miller, E.M. Stolper, T.J. Ahrens, The equation of state of a molten komatiite 1. Shock wave compression to 36 GPa, J. Geophys. Res. 96 (1991) 11831–11848.
[21] J.E. Reid, B.T. Poe, D.C. Rubie, N. Zotov, M. Wiedenbeck, The self-diffusion of silicon and oxygen in diopside ($CaMgSi_2O_6$) liquid up to 15 GPa, Chem. Geol. 174 (2001) 77–86.
[22] J.E. Reid, Transport Properties of Silicate Liquids at High Pressure, Ph.D. Thesis, University of Bayreuth, 2002.
[23] E.R.G. Eckert, Introduction to the Transfer of Heat and Mass, McGraw-Hill, New York, 1950, 284 pp.
[24] A.J. Chapman, Heat Transfer, Macmillan, New York, 1974, 653 pp.
[25] K. Righter, M.J. Drake, Formation of eucrites and diogenites during equilibrium crystallization of a magma ocean on a Vesta-sized asteroid, Meteorit. Planet. Sci. 32 (1997) 929–944.
[26] G.F. Davies, Heat and mass transport in the early Earth, in: H. Newsom, J.H. Jones (Eds.), The Origin of the Earth, Oxford Press, London, 1990, pp. 175–194.
[27] J. Crank, The Mathematics of Diffusion, Oxford University Press, Oxford, 1975, 414 pp.
[28] R. Gunn, G.D. Kinzler, The terminal velocity of fall for water droplets in stagnant air, J. Meteor. 6 (1948) 243–248.
[29] H. Rouse, Elementary Mechanics of Fluids, Dover, New York, 1978, 376 pp.
[30] S. Chandrasekhar, Hydrodynamic and Hydromagnetic Stability, Oxford, New York, 1961, 652 pp.
[31] G.A. Young, The Physics of the Base Surge, U.S. Naval Ordnance Laboratory, 1965.
[32] K. Righter, M.J. Drake, Effect of water on metal-silicate partitioning of siderophile elements: a high pressure and temperature terrestrial magma ocean and core formation, Earth Planet. Sci. Lett. 171 (1999) 383–399.
[33] D.P. Dobson, J.P. Brodholt, L. Vocadlo, W.A. Crichton, Experimental verification of the Stokes-Einstein relation in liquid Fe-FeS at 5 GPa, Mol. Phys. 99 (2001) 773–777.
[34] D.P. Dobson, Self diffusion in liquid Fe at high pressure, Phys. Earth Planet. Int. 130 (2002) 271–284.
[35] D.L. Turcotte, G. Schubert, Geodynamics, John Wiley, New York, 1982, 450 p.
[36] A. Suzuki, E. Ohtani, T. Kato, Density and thermal expansion of a peridotite melt at high pressure, Phys. Earth Planet. Int. 107 (1998) 53–61.
[37] T.J. Ahrens, K.G. Holland, G.Q. Chen, Phase diagram of iron, revised-core temperatures, Geophys. Res. Lett. 29 (2002) 10.1029/2001GL014350.